Solar and Stellar Physics Through Eclipses
ASP Conference Series, Vol. 370, 2007
O. Demircan, S. O. Selam & B. Albayrak

Damping of MHD Waves as a Heating Mechanism of Solar Corona

S. Nasiri[1,2] , H. Safari[1], and Y. Sobouti[1]

[1]*Institute for Advanced Studies in Basic Sciences (IASBS)*
P.O. Box 45195-1159
[2]*Department of Physics, Zanjan University, Zanjan, Iran*

Abstract. Damping of MHD waves seems to play an important role in heating the solar corona. In this respect a magnetized flux tube with a specified density profile is considered and the singularity of ideal equation of motion in coronal approximation is removed by introducing the viscous and resistive damping in the tube. The resultant equations are solved by applying the connection formula technique. The damping rates are obtained for both inside and outside of the resonance layer and are commented on. Next, the same problem that undergoes a longitudinal density stratification is considered. Equations of motion are expressed by second order differential equations that are separable into radial and transverse components. The radial equation is solved in thin tube approximation, while the transverse one is solved numerically.

1. Introduction

Ionson (1978) was first to suggest that the resonant absorption of MHD waves in coronal plasmas could be a primary mechanism in coronal heating. Since then, much analytical and numerical work has been done on the subject. In the absence of resonance, Edwin & Roberts (1983) and Roberts et al. (1984) introduced a formalism that is applicable to the solar coronal oscillations. Karami et al. (2002; hereafter paper I) studied the full spectrum of MHD modes of oscillations in zero-β magnetic flux tubes with discontinuous Alfvén speeds at the tube's surface. In the vicinity of singularity, field gradients are large. Recognizing this, Safari et al. (2006; hereafter paper II) used Sakurai et al. (1991) and Goossens et al. (1995) method and analyzed the dissipative processes in such regimes. The frequency shift in the fundamental and first harmonic transverse oscillations in the coronal loops was first observed by Verwichte et al. (2004). Possible factors that cause the shift in frequency and change the oscillation properties of the loop are investigated by different authors. The effects of slow variations of the cross sectional area on the oscillations of a loop is investigated by Nasiri (1992). Van Doorsselaere et al. (2004) investigated the effect of longitudinal curvature on quasi modes of a typical coronal loop. They found that the frequencies and damping rates of ideal quasi modes were not influenced much by the curvature. Andries et al. (2005) studied the effect of density stratification on coronal loop oscillations, and conclude that longitudinal mode numbers are coupled due to the density stratification. Here, we use analytical and numerical methods to understand the effect of the longitudinal density variation on the coronal loops oscillations.

The layout of the paper is as follows: In Sec. 2. the equations of motion, the resonance absorption and coronal loop oscillations in thin layer approximation are included. In Sec. 3. the effect of longitudinally density stratification on coronal loop oscillations are presented. Concluding remarks are devoted to Sec. 4.

2. Equations of Motions

The linearized MHD equations for a zero-β, but resistive and viscous plasma are

$$\frac{\partial \delta \mathbf{v}}{\partial t} = \frac{1}{4\pi\rho}\{(\nabla \times \delta\mathbf{B}) \times \mathbf{B} + (\nabla \times \mathbf{B}) \times \delta\mathbf{B}\} + \frac{\eta}{\rho}\nabla^2 \delta\mathbf{v}, \tag{1}$$

$$\frac{\partial \delta \mathbf{B}}{\partial t} = \nabla \times (\delta\mathbf{v} \times \mathbf{B}) + \frac{c^2}{4\pi\sigma}\nabla^2 \delta\mathbf{B}, \tag{2}$$

where $\delta\mathbf{v}$ and $\delta\mathbf{B}$ are the Eulerian perturbations in the velocity and the magnetic fields; ρ, σ, η and c are the mass density, the electrical conductivity, the viscosity and the speed of light, respectively.

2.1. Resonance absorption and coronal loop oscillations

We first assume that the equilibrium density is a function of r only, $\rho(r)$. In the next section we relax this restriction and assume a longitudinal density stratification. A constant magnetic field is assumed along the z axis, $\mathbf{B} = B\hat{z}$. It is also assumed that there is no initial steady flow inside or outside of the tube and the density scale heights are much larger than the dimensions of flux tube, so that the gravity stratification is negligible. Viscous and resistive coefficients, η and σ respectively, are constants. For a variable density, $\rho(r)$, a singularity develops wherever the local Alfvén frequency becomes equal to the global frequency of the mode. The relevant radial wave number vanishes and resonant absorption takes place. Let us denote the radius of the tube by R and a radius beyond which the resonance occurs by $R_1 < R$. The thickness of the inhomogeneous layer, $a = R - R_1$, will be assumed to be small and will be arbitrarily taken to be of the order of $R/10$. The choice of density profile is also unimportant. We will assume constant density, ρ_i, in $0 \leq r \leq R_1$; a second constant density; $\rho_e < \rho_i$, in $r \geq R$; and linearly decreasing density in $R_1 \leq r \leq R$. In $r < R_1$ and $R < r$, viscosity and resistivity will be neglected and solutions of Eqs. (1) and (2) will be taken from paper I. In $R_1 < r < R$, within which the singularity occurs, viscosity and resistivity will be restored and solutions will be found by expanding Eqs. (1) and (2) about the singular point. Finally, interior and exterior solutions will be connected with those of the resonant layer by connection formulae of Sakurai et al. (1991a)

2.2. Dispersion relation and damping rate

From paper I and II, in the absence of dissipations, all components of $\delta\mathbf{v}$ and the transverse components of $\delta\mathbf{B}$ are expressible in terms of δB_z only. The latter, in turn, is the solution of a second order differential equation. Thus,

$$\frac{k^2}{r}\frac{d}{dr}\left[\frac{r}{k^2}\frac{d\delta B_z}{dr}\right] + (k^2 - \frac{m^2}{r^2})\delta B_z = 0, \tag{3}$$

where $k^2=\omega^2/v_A^2-k_z^2$, and $v_A(r)=B/\sqrt{4\pi\rho(r)}$ is the local Alfvén speed. Here we have assumed an exponential ϕ, z and t dependence, $exp[i(m\phi+k_z z-\omega t)]$ for any component of $\delta\mathbf{v}$ and $\delta\mathbf{B}$.

In the interior region, $r\leq R_1$, solutions of Eq. (3) are

$$\delta B_z=\begin{cases} I_m(|k_i|r), & k_i^2<0, \quad r\leq R,\\ J_m(|k_i|r), & k_i^2>0, \quad r\leq R, \quad k_i^2=\omega^2/v_{A_i}^2-k_z^2,\\ K_m(k_e r), & k_e^2=k_z^2-\omega^2/v_{A_e}^2>0, \quad r>R, \end{cases} \tag{4}$$

where J_m, I_m, and K_m are Bessel and modified Bessel functions of the first kind, and the second kind, respectively. The jump conditions across the boundary for δB_z and δv_r are (see paper II)

$$[\delta B_z]=0, \tag{5}$$

$$[\delta v_r]=-\pi\tilde{\omega}\frac{1}{|\Delta|}\frac{m^2}{\rho(r_A)r_A^2}B_z\delta B_z. \tag{6}$$

Here $R_1<r_A<R$, is the radius at which the singularity occurs and $k^2(r_A)=0$; $\tilde{\omega}=\omega+i\gamma$, where γ is the damping rate; and $\Delta=-B^2\frac{d}{dr}(\frac{k^2}{\rho})|_{r_A}$. Substituting the fields of Eq. (4) in jump conditions and eliminating the arbitrary amplitudes of the wave, foreseen initially inside and outside of the boundary layer, gives the dispersion relation

$$-\frac{1}{k_e}\frac{K_m'(|k_e|R)}{K_m(|k_e|R)}+\frac{1}{k_i}\frac{J_m'(|k_i|R_1)}{J_m(|k_i|R_1)}-i\pi\frac{1}{|\Delta|}\frac{m^2}{\rho(r_A)r_A^2}=0. \tag{7}$$

In principle $\tilde{\omega}=\omega+i\gamma$ is expected to be found as a solution of Eq. (7). In particular for $\gamma\ll\omega$ and thin boundary approximation, which assumes $(R-R_1)/R=a\ll 1$, Eq. (7) can be expanded to give damping rate (see paper II)

$$\gamma \;=\; -\left\{\frac{\pi m^2}{\omega_{nml}^2(\rho_i-\rho_e)}\frac{a}{R^2}\right\}\Big/\frac{d}{d\omega}\left\{\frac{1}{k_e}\frac{K_m'(|k_e|R)}{K_m(|k_e|R)}\frac{1}{k_i}\frac{J_m'(|k_i|R)}{J_m(|k_i|R)}\right\}. \tag{8}$$

The results for surface waves are the same as those for body waves except that J_m is replaced by I_m. The two waves exhibit differences, for J_m and I_m behave differently at the boundary. We also note that each surface mode is designated by only two wave numbers, (m,l) corresponding to ϕ and z directions, respectively. As typical parameters for a coronal loop, we adopt radius $=10^3$ km, length $=10^5$ km, $\rho_i=2\times10^{-14}$ gr cm^{-3}, $\rho_e/\rho_i=0.1$, $B=100$ G. For this parameter one finds $v_{A_i}=2000$ km s^{-1}, $v_{A_e}=6400$ km s^{-1} and $\omega_A=2$ rad s^{-1}.

In Fig. 1 the frequency, ω_{nml}, and the spectral damping rate, $\gamma_{nml}/\omega_{nml}$, for body waves are plotted versus l. The frequency increases with increasing n and l. For $(n,m)=(1,1)$, the spectral rates have a minimum at $l\approx 15$ and a maximum at $l\approx 45$. For $(n,m)=(2,1)$, the minimum is cut off and the maximum is shifted to $l\approx 75$. For $(n,m)=(3,1)$ both minimum and maximum are cut off and there is only a declining branch. The reason for decreasing rates at higher l values is the shift of the maximum amplitude of waves away from the boundary layer towards the axis of the tube. For surface waves, specified by two

mode numbers (m, l), ω_{ml} and γ_{ml}/ω_{ml} of a thick and thin tube are presented in Paper II. The inverse of the spectral rate is the number of oscillations taking place before the wave is completely attenuated. For thick and thin tubes, and $m = 1$ and $1 \leq l \leq 10$, this number is about 1.6 and 4.8, respectively (Safari et al. 2006). The observed values of Nakariakov et al. (1999) and Goossens et al. (2002) from TRACE data, are 3 or 4.

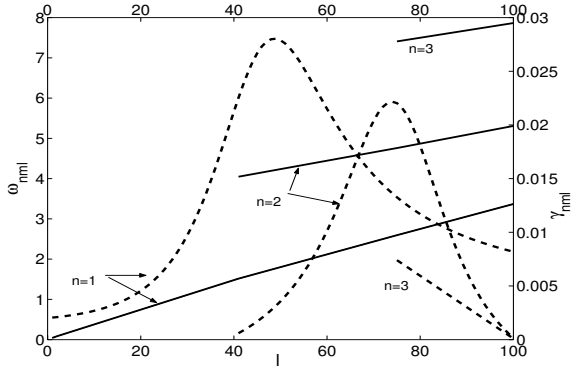

Figure 1. Body modes: ω_{nml} (solid lines) and γ_{nml} (dashed lines) versus l for $m = 1$ (kink) modes. Auxiliary parameters are: the tube radius 10^3 km, the tube length 10^5 km, $B = 100$ G, $\rho_i = 2 \times 10^{-14}$ grcm^{-3}, $\rho_e/\rho_i = 0.1$. Frequencies are in units of the interior Alfvén frequency, $\omega_A = 2$ rad s^{-1}.

3. The Effect of Longitudinal Density Stratification on Coronal Loop Oscillations

In this section, we are interested in the effects of density stratification with height $\rho_i(z)$ and $\rho_e(z)$ for the interior and exterior of the loop, respectively. Time and ϕ- dependence for perturbed quantities is $exp[-i(\Omega t - m\phi)]$ and the dissipative terms are neglected. With these assumptions, Eqs. (1) and (2) give the following equation for δB_z

$$\left(\frac{1}{r}\frac{\partial}{\partial r}r\frac{\partial}{\partial r} + \frac{\partial^2}{\partial z^2} - \frac{m^2}{r^2}\right)\delta B_z + \frac{\Omega^2}{v_A^2}\delta B_z = 0. \tag{9}$$

This is a wave equation for δB_z with the variable speed $v_A(z)$. It could be solved by the separation of variables. Let

$$\delta B_z = \Psi(r)Z(z). \tag{10}$$

Equation (9) splits into

$$\left(\frac{d^2}{dr^2} + \frac{1}{r}\frac{d}{dr} - \frac{m^2}{r^2}\right)\Psi(r) + k^2\Psi(r) = 0, \quad k^2 = \frac{\Omega^2}{v_A^2|_{\epsilon=0}} - \kappa_z^2, \tag{11}$$

$$\left(\frac{d^2}{dz^2} - k^2\right)Z(z) + \frac{\Omega^2}{v_A^2}Z(z) = 0, \tag{12}$$

where ϵ is the scale height and is in Eq. (13). Each of Eqs. (11) and (12) are actually a pair for inside and outside of the tube. They are to be solved simultaneously for the values of $\Psi(r)$, Z, κ_z, and Ω.

We assume

$$\begin{aligned} \rho(\epsilon, z) &= \rho_i(\epsilon) f(\epsilon, z), \qquad r < a \\ &= \rho_e(\epsilon) f(\epsilon, z), \qquad r > a \end{aligned} \tag{13}$$

where $\rho_i(\epsilon)$ and $\rho_e(\epsilon)$ are the interior and exterior densities at the footpoints and a is the radius of the loop. In the approximation of an isothermal loop in a constant gravity, $f(\epsilon, z) = exp(-\frac{\epsilon}{\pi} \sin \frac{\pi z}{L})$, $\epsilon = L/H$, and H is the scale height. Interior solutions of Eq. (11) are the same as in Eq. (4). Imposing the boundary conditions of paper I give

$$\frac{1}{k_i} \frac{J'_m(|k_i|R)}{J_m(|k_i|R)} - \frac{1}{k_e} \frac{K'_m(|k_e|R)}{K_m(|k_e|R)} = 0, \tag{14}$$

Here we study Eq. (14) for thin stratified loops by numerical techniques. For $a/L \ll 1$ and $m \geq 1$ the dispersion relation of Eq. (14) gives

$$\Omega = \kappa_z B [2\pi(\rho_i(0) + \rho_e(0))]^{-1/2}. \tag{15}$$

See also Edwin & Roberts (1978), Hasan & Sobouti (1987), Karami et al. (2002), Van Doorsselaere et al. (2004), Díaz et al. (2004). Substituting Eq. (15) in Eq. (12) yields

$$\begin{aligned} \frac{d^2 Z}{dz^2} + \frac{4\pi\Omega^2}{B^2} \frac{\rho_i(0) + \rho_e(0)}{2} F(\epsilon, z) Z(z) &= 0, \ F(\epsilon, z) \\ &= \frac{2\rho_i(\epsilon, z) - \rho_i(0) + \rho_e(0)}{\rho_i(0) + \rho_e(0)}. \end{aligned} \tag{16}$$

Using a numerical code, based on shooting method, Eq. (16) is solved for eigenvalues and eigenfunctions. In Fig. 2 the fundamental and the first overtone frequencies, Ω_1 & Ω_2, respectively, and their ratio are plotted as functions of ϵ. Both frequencies show monotonous increase with increasing ϵ. For small ϵ's Ω_1 has a steeper slope than Ω_2, but both approach each other as ϵ increases. The ratio P_1/P_2 begins at 2 for $\epsilon = 0$ and decreases to one at large ϵ's. The longitudinal part of the eigenfield, $Z(z)$, is plotted in Figs. 2. For odd l values as ϵ increases the middle antinode gradually flattens and eventually bifurcate into two humps with a dip in between. For both $l = 1$ & 3 this happens for $\epsilon \geq 3\pi$. The larger the epsilon the deeper the dip becomes. For both even and odd l's, the antinodes move towards the footpoints and away from each other with increasing ϵ.

4. Concluding Remarks

In this paper we studied the effects of damping MHD waves on the modal structure of a magnetized flux tube. The presence of the viscous and resistive dissipations remove the singularity in the ideal differential equations of motion.

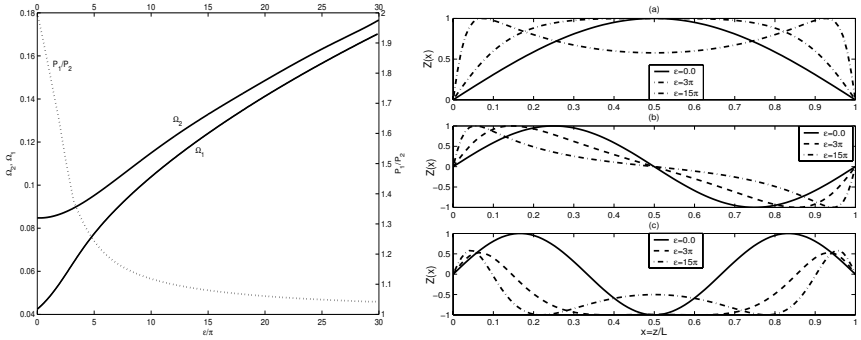

Figure 2. Left: The frequencies, Ω_1 and Ω_2, and the ratio of P_1/P_2, are plotted versus ϵ/π. Auxiliary parameters are: the tube length $100a$, B = 100 G, and density contrast $\rho_e/\rho_i = 0.1$. Right: a) The fundamental modes ($l = 1$), b) the first overtone modes ($l = 2$), and c) the second overtone modes ($l = 3$), for non-stratified, $\epsilon = 0$, and stratified, $\epsilon/\pi = 3,\ 15$, versus z.

The solutions are obtained by applying the connection formula technique to the boundaries of the thin resonance layer located inside the tube and undergoing an appropriate boundary conditions. The damping rates obtained are in agreement with the data obtained by the TRACE. We also considered a longitudinally density stratified flux tube and solved the corresponding linearized differential equations of motion both by perturbation theory and by numerical analysis. Our results for realistic values of the coronal loops parameters are in agreement with those obtained by the observations.

Acknowledgments. This work was supported by the Institute for Advanced Studies in Basic Sciences (IASBS), Zanjan.

References

Andries, J., Goossens, M., Hollweg, J. V., Arregui, I., & Van Doorsselaere, T. 2005a, A&A, 430, 1109
Díaz, A. J., Oliver, R., Ballester, J. L., & Roberts, B. 2004, A&A, 424, 1055
Edwin, P. M., & Roberts, B. 1983, Sol. Phys., 88, 179
Goossens, M., Hollweg, J. V., & Sakurai, T. 1992, Sol. Phys., 138, 233
Goossens, M., Andries, J., & Aschwanden, M. J. 2002, A&A, 394, L39
Hasan, S. S., & Sobouti, Y. 1987, MNRAS, 228, 427
Ionson, J. A. 1978, ApJ, 226, 650
Karami, K., Nasiri, S. & Sobouti, Y. 2002, A&A, 396, 993
Nakariakov, V. M., Ofman, L., Deluca, E. E., Roberts, B., & Davila, J. M. 1999, Science, 285, 862
Nasiri, S. 1992, A&A, 261, 615
Roberts, B., Edwin, P. M., & Benz, A. O. 1984, ApJ, 279, 857
Safari, H., Nasiri, S., Karami, K., & Sobouti, Y., 2006, A&A, 448, 375.
Sakurai, T., Goossens, M., & Hollweg, J. V. 1991a, Sol. Phys., 133, 247
Van Doorsselaere, T., Debosscher, A., Andries, J., & Poedts, S. 2004, A&A, 424, 1065
Verwichte, E., Nakariakov, V.M., Ofman, L., & DeLuca, E.E. 2004, Sol. Phys., 223, 77